Colorado Space Grant Consortium

Balancing Motion and Biology: Payload Stabilization and Blood Integrity in Near-Space Flight

Sirius

Buffington, R., David, J., Zubrod, M., Schick, B., & Mackenzie, O. (2026). COSGC DemoSat.

Front Range Community College – Boulder County Campus. Instructor: Anthony Riley

1 Abstract 2
2 Introduction 2
2.1 Project Overview 2
2.2 Background 3
2.3 Payload Requirements 3
3 Procedure, Design, and Reasoning 4
3.1 Blood Procedure and Reasoning 4
3.2 Shell Design and Reasoning 5
3.3 Gyro Design and Reasoning 7
4 Preliminary Review and Predictions 10
4.1 Bringing It All Together 10
4.2 Blood Predictions 11
4.3 Gyro Review and Predictions 12
4.4 Shell Review and Predictions 12
5 Flight Day 13
6 Conclusion 14
6.1 Blood 14
6.2 Flywheel System and Payload Design 15
6.3 Other Data and Correlations 17
7 Reflection 18
7.1 Future Iterations and Studies 18
8 Appendices 20
9 References 32

[1.0] Abstract

While humanity dreams of the stars, our bodies have biological limits. Safe payloads transporting people and delicate biological materials remain a critical challenge, requiring stabilization and protection to ensure flight safety. The Sirius team created a stabilization gyro that reduces the centripetal force due to wind and overall rotational acceleration, increasing safety for sensitive materials. The team also crafted a shell for the payload, which was created with the intent of reducing the effects of altitudes near the upper atmosphere on the payload, protecting against high-impact forces. The biological material used to test the payload protection was blood, which was studied to analyze the effects of near-space radiation, pressure, and temperature. The team formulated two hypotheses: the overall dosage from the flight would have little to no effect on red blood cell count while having a small effect on the number of white blood cells; the combination of the fabricated hull and stabilization system would drastically decrease the rotation experienced by the payload during flight. While the tests did conclude that there was a reduction in potential rapid rotation as provided by the stabilization system, there was substantial damage to the blood as a result of the mechanical shock upon touchdown of the Sirius project. Additionally, the stabilization of the project was improved drastically by the onboard systems.

[2.0] Introduction

[2.1] Project overview

This project focuses on designing and developing a self-contained platform that collects environmental data during high-altitude flight and stabilization. The system integrates multiple sensors, onboard data logging, blood vials, a uniquely fabricated hull, and an active and passive stabilization mechanism to collect accurate data throughout the flight. One of the primary goals of this payload is to measure and record the levels of radiation exposure during high-altitude flights. At higher altitudes, the Earth's atmosphere provides less of a shielding effect, allowing increased levels of high-energy particles to reach the payload. Monitoring the biological specimen during these changes in radioactive exposure provides insight into how irradiation severity varies with altitude, due to atmospheric density decreasing, and how these variables can affect human blood. The Sirius team sent up two vials of human blood, maintaining two control samples on the ground for comparison.

One of the largest concerns when transporting delicate materials, such as blood, is the prevention of shock and excessive rotational force. To minimize uncontrolled rotation, which would prevent centrifugal separation and damage caused by acceleration, the platform incorporates an active and passive correction wheel system. When the gyroscope detects rotational motion outside of an allowed tolerance band, the control system sends a signal to one of the DC motors to begin to spin up and the stabilization loop begins. Whilst in either passive or active modes, all systems are designed to run autonomously for extended periods during flight. This correction system is aided by the overall design and fabrication of the payload hull. This project incorporates mechanical design, embedded electronics, structural design and fabrication, sensor systems, and biological integration to create a compact scientific instrument capable of operating in a high-altitude environment.

[2.2] Background

The study of biological materials, such as blood, in space or near space, is a subject that has not been extensively researched and is a topic that NASA, among others, has started to develop testing plans for. A previous Colorado Space Grant team (University of Colorado Boulder, Colorado Space Grant Consortium (2023)) had conducted an experiment associated with the effects of flight blood but were entirely focused on the change of pH and viscosity, unlike what the Sirius project was focused on. This specific issue is solved by the utilization of various stabilization techniques.

The ability to combine enhanced payload stabilization, while being under a tight mass constraint, is a challenge that many previous teams have attempted, with many being successful in correcting rotation by up to 53.99%. (University of Colorado Boulder, Colorado Space Grant Consortium, 2025) This percentage is based on a calculation utilized by a previous team from CSU. (see [16. 6.2]). The fabricated shell, used as the hull, is unique to the Sirius project. (see [Figure 3.2]).

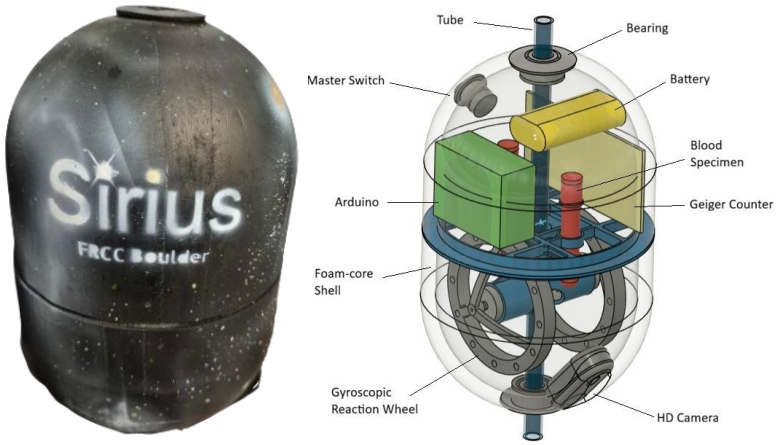

Figure 1

[2.3] Payload requirements

The Teams' primary budgets were a 600g mass budget and a monetary budget of $800. The payload must also meet the safety requirements required due to the use of Biohazards; medical safety (see [4, Sec. 3.1]), mechanical safety requirements such as minimal torque on the string holding the payload, and size requirements (see [6, Sec. 3.2] and [10, Sec. 3.3.3]).

[3.0] Procedure, design and reasoning

[3.1] Blood Procedure and Reasoning

The biological material that the Sirius project utilized for this experiment was blood. To ensure a safe flight, landing, recovery, and replicable results, flight safety must be maintained. The blood was contained in a CBC lavender top 4.0 mL vial [see figure 2] to prevent leakage into the vacuum casing and stored inside a plastic biohazard bag. The team tested four samples, two sent up in the payload, and two used as a control sample. The four samples were provided by two separate donors.

Figure 2

One of the concerns associated with using blood in this experiment was the containment associated with the usage of biological matter. Care was taken to ensure that the blood did not leave the casing during the flight via proper containment. The spillage of biological material in potential landing zones, such as private property, public areas, or farms, was the main concern for this section of the experiment. Temperature was another factor considered during these tests, as temperature fluctuations can vary by large margins as the payload rises in altitude. Wide swings in temperature can cause a myriad of different issues when handling blood. Blood freezing can cause hemolysis, weaken red blood cell membranes, and make the cell more susceptible to damage. Thus, the blood was kept above 0 °C to prevent freezing before and during the flight. While no active heating was utilized during the flight, the location in which the blood was stored allowed for the heat generated by the motors to provide protection from freezing (see [12, Sec. 4.3]).

The next concern for the Sirius team was to ensure that the blood utilized in the testing was drawn safely. To achieve this goal, the blood was drawn by a registered EMT supported by a team member. Using a Peripheral venous catheter, blood was drawn into the Caples using gravity (see [Figure 3.]). Then the catheter was safely removed, and a bandage was applied to the wound. The method used to test the blood was a medical standard CBC, or Complete Blood Count test, conducted by Boulder Community Health. The CBC test was chosen due to its low cost compared to other tests, such as radiation dosimetry or DNA analysis. The CBC test also provided the benefit of being able to be tested in a medical standard laboratory and schedule flexibility was available due to the willingness of the staff present.

Figure 3

The Sirius project team did have to manage a deadline set by the testing laboratory for the CBC testing. The blood was required to be provided to the lab within 24 hours of being drawn to provide the most accurate tests, due to the quick degradation of blood outside of the body. This was accomplished by tracking the exact time that the blood was drawn immediately before flight, with the blood being delivered to the laboratory on the same day that it was drawn. The Sirius team drew the four samples at 4:30 am on April 4th, 2026 [see Figure 3]. The blood was secured in the payload and, when recovered, the

blood was kept in biohazard bags until it was provided to the hospital at 2:01 pm on April 4th, 2026, for the CBC test.

All procedures involving human blood were approved by Front Range Community College, and permission for flight for a Biohazard level 2 was given by Annie Strange, director of the Colorado Space Grant Consortium. Informed consent was granted by blood donors, who were told of the study's aims, procedures, and risks. Blood collection and handling followed Biosafety level 2 protocols, including the use of sterile equipment, secure and safe storage, and laboratory access. Human blood was necessary to simulate physiological conditions and effects on the blood, and no alternative was found. For questions about procedure and safety protocols, please contact Dr. Annie Strange at annie.strange@colorado.edu.

[3.2] Shell design and reasoning

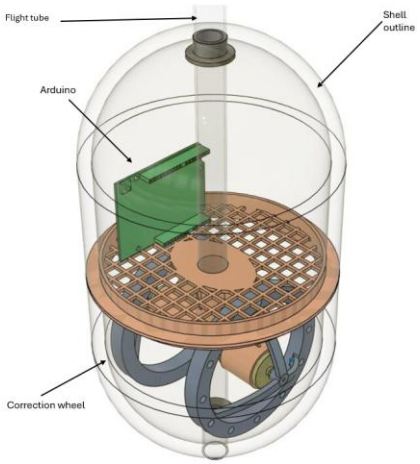

Figure 4

To achieve payload stabilization, the hull design needed to mitigate any forces that could apply torque to the payload and induce rotation. Potential torque comes from two main sources: the shape of the craft and drag as it moves through the air, and the rotation and twisting of other payloads on the flight string. At the same time, the craft must be able to rotate to take advantage of the stabilizing torque produced by the gyroscopes. For these reasons, the hull was designed to be aerodynamic, isolated from the launch tether, and free to rotate for overall stabilization.

The hull's pill shape, with minimal projections and recesses for airflow to catch, was the primary approach for improving aerodynamic stability. The craft was isolated from the launch tether using a pair of 3D-printed bearings: the inner diameter being fixed to the central tether tube, while the outer diameter attaches to the hull, allowing the payload to rotate freely.

Each half of the hull is built from three components: an inner shell, an outer shell, and a foam core. The inner and outer shells are each made from two layers of ultra-light polyester garment fabric. Polyurethane glue is applied between the layers, and the assembly is vacuum-pressed over a 3D-printed form using a standard kitchen vacuum-seal bag. After curing for about 8 hours, the shells are removed from the bag and released from the mold. The completed inner and outer shells are then spaced 10 mm apart, and the cavity between them is filled with insulating spray foam.

The finished material is lightweight and strong, absorbs impact forces, and provides excellent insulation for the temperature-sensitive payload. It can be cut with a knife or saw or machined with an electric router or Dremel rotary tool. The material also sands easily, and paint adheres to it well.

After creating the design in CAD (see [Figure 4]), the Sirius team created a prototype using Fused Deposition Modeling (FDM) 3D printing. During testing, the Sirius team identified three primary problems. First, the Sirius team found that using FDM printing created points of structural failure along the layer line. When force was applied parallel to these layer lines, the shell was more likely to fail or collapse. Secondly, through impact testing, it was found that the shell could not absorb the blunt force to the tolerance needed. And last, the shell weighed over 240 grams. Due to these identified issues, a new material was required to be utilized as a hull. A new material was then created that could hold its shape and absorb force applied to it. It used a double layer of polyester fabric, with a foam core created by spraying foam on the inside of one of the fabric pieces. Utilizing two 3-D molds, the shape of the hull was formed by the compression between them and the fabric pieces being held stable against the expanding foam (see [Figure 5]).

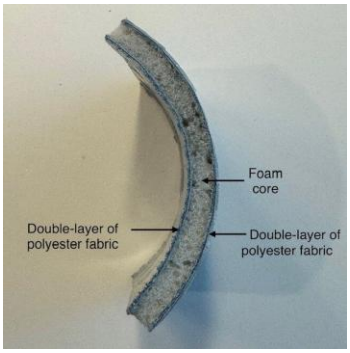

Figure 5

The payload was attached to a string, which was initially chosen for the gyro to produce enough torque to stabilize the payload. However, it was decided that the resulting force applied by the rotation of the other projects would be significant, which prompted the Sirius team to search for a solution to remove said external force. A 3-D printed ball bearing centered around the flight tube was designed and printed because of this conclusion. This also provided a way to apply torque on the payload without subsequently twisting the string.

Then, using a 3d printed mold and using methods above to create the shell material, two molds were created, one for the top half and one for the bottom half. Then using the motor housing as a connector (See [8, Sec. 3.3.1]), the two halves were bonded to the motor housing using hot glue and the remaining gap between the top and bottom half sealed with aluminum tape (see [Figure 6]).

Figure 6

[3.3] Gyro design and reasoning

[3.3.1] Design overview

To minimize uncontrolled rotation, the platform incorporated an active and passive correction wheel system. During the active correction, when the gyroscope detected unwanted rotational motion, the microcontroller commanded one DC motor and its associated weighted flywheel to accelerate or decelerate their coupled reaction wheels to mitigate rotation. This system provided a mechanism to introduce controlled torque output to the payload and was designed to run autonomously for extended periods during flight. This subsystem had 4 main aspects that process communications and create stabilization. This system has undergone multiple interactions, with the overarching design process discussed in depth further below.

[3.3.1] Motor flywheel braking system

Figure **7**

For this first step in the design process, there was one flywheel that would spin clockwise or counterclockwise to provide correction to payload. This wheel provided correction based on the conservation of angular momentum $L = I\omega$ where I is the moment of inertia and ω is the angular velocity. When the motor accelerates the flywheel, it applies to a torque that increases the wheels' angular momentum and thus, due to Newton's Third Law, an equal and opposite torque is applied to the payload. As a result, the payload rotates in the opposite direction; the flywheel is spinning. Through this interaction, the flywheel system provided a basic means of correction. When the system detected unwanted rotation (See [10, Sec. 3.3.3]), the wheel began to accelerate in the opposite direction. But, to produce the strongest torque, the flywheel must have the greatest mass possible and as large as possible, as seen by the following equation. To provide a stronger torque, small metal balls were added to the inside edges of the flywheel (see [Figure 7]).

Figure 8

After initial testing of this iteration using a single wheel gyro, it was found that when the wheel would switch correction directions, the built-up momentum prevented the wheel from quickly correcting in the opposite direction (see [Figure 8]). This would often lead to a cycle of continuous over-correction, as the system would try to correct the motion that it itself induced in the overall system. As a solution to this issue, in Version 2 the team created a circular housing to fit the shell (See [5, Sec 3.2]) and added another motor to provide better correction when rapidly switching directions.

Figure 9

The Sirius team also tested having the motors at a 120-degree angle from the base to both better fit within the shell and to be able to apply torque along varying axes However, in order to have the motors canted at an angle, the overall structure would see an increase of approximately 10 grams. This added mass was deemed too high, and the team decided to keep the motors fixed in parallel at a 90-degree angle from the base of the support structure. As a last change, the solid plate of the structural support was changed to a beam design with two open holes to contain the blood vials, which saved a considerable amount of mass in the final product (see [Figure 9]).

[3.3.2] Power system and circuit design

To begin, a 9V source was used to supply power to the Arduino Uno R4, accelerometers, and a D.C. motor. An issue was encountered when attempting an initial stabilization test; the accelerometer and the motor would begin to read an incorrect constant value, which would result in the motor continuously running. It was also found that the fewer corrections performed by the motor, the longer the correction would last before reading an incorrect result. As a result, instead of using raw gyroscope data, integrated libraries were utilized as an alternative. To use libraries, components from Adafruit were chosen with the best documentation as to how to use their libraries with the base Arduino code (see [9, Sec. 3.3.3]). After making these changes, an oscilloscope was used to test the wires to determine if the data was correctly being sent, which confirmed that the wires were sending the correct data. Along with verifying that the data was being correctly sent, there did exist a large amount of ‘noise’ along these wires. To reduce this noise, the longer connector wires were wrapped with insulative materials to prevent induced voltages from the magnetic fields created by the current running through the other wires.

The second set of ideas proposed included adding a second motor to serve as a brake (see [7, Sec. 3.3.1]). The goal in utilizing the second motor was that the spinning of the second motor in the opposite direction would stop the first motor from gaining too much momentum and overcorrecting with excessive rotational force. To accomplish this, a second DC motor was added, and the path for data logging was added to an SD card. Live data transmission was also accomplished but was limited to a certain height by the strength of the data transmitter and federal law restrictions. Due to this limitation, SD card logging was established as the base method for data collection in this project. An SD card shield was added to the

Arduino as it allowed for easier insertion and removal of the SD card as well as providing additional ports for wires to be connected for use in the future.

Figure 10

The last addition to the Arduino system was that of a motor/stepper/servo shield. This allowed the project to implement motor, stepper, and servo drivers without requiring an external connection outside of the overall Arduino system. The shield also came with the added benefit of having screw in terminal connectors (see [Figure 10]) which allowed for quick connection and disconnection from the motors, streamlining assembly and testing.

A Geiger counter was connected to the motor shield to read the radioactive exposure values experienced during the flight. A gyroscope and accelerometer were connected along the same wire directly to the Arduino, to which the pressure/humidity/temperature sensor was also connected. The final connection made to the Arduino system was an 8000 mAh battery (see [Figure 11]).

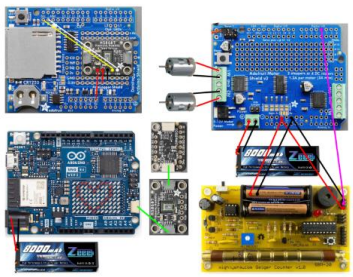

Figure 11

[3.3.3] Arduino and software

This subsystem uses both active and passive correction phases. Both modes use a LSM6DSOX IMU, which finds the DEMOSAT Z-axis rotation. During calibration, the system sets up a baseline by averaging 500 samples to calculate gyroZ, ensuring that any later movement is measured against a true "still" state. During Active correction, which uses a closed-loop feedback approach. the system begins to experience rotation in the z axis. The proportional-integral-derivative (PID) algorithm begins to calculate the correction value (pwnCORR). The Proportional term (set at 2.0) = k_p provides an immediate response scaled to the spin speed, while the Integral term (0.5) = k_i slowly builds power to cut

persistent low-speed drifts, though it is constrained to a value of ±50 = $e(t)$ to prevent the motor from over-reacting. The Derivative term (2.0) = k_d acts as a damper, predicting when the DEMOSAT is nearing its target and slowing the motor to prevent overshooting.

$$\text{PWMCORR(t)}=K_p e(t) + ki \int_0^t e(\text{T}) d\text{T} + K_d \frac{de(t)}{dt}$$

Following the active correction phase, after an hour the system transfers to passive correction. In this phase, the system identifies a "stability window", defined as rotation rates under 2.0 degrees per second, yet with the primary correction motor still exerting rotation at a high rate over 150pwm. If this condition is met the program defines it as momentum saturation, where the flywheel has reached its

acceleration limit. This activates the secondary motor which begins to spin in the opposite direction of the first wheel, removing excess rotational energy as it approaches 10 degrees. This slows the payload, so the project does not overshoot the rotation and cause continuous oscillation.

$$\left|\omega_z^{filtered}\right| < 2.0 \frac{deg}{s} \quad , \quad |u(t)| > 150\, PWM$$

Both active and passive correction phases provide a controlled stabilization process. Active correction should provide dynamic closed-loop feedback for precise stabilization, while passive correction was a secondary test to see if stabilization could be achieved in an open loop, low processing format to compare the two.

The Audino also continuously logs environmental, inertial, radiation, and actuator data. All these transitions are logged at 12Hz to the SD card and temporarily provided over Wi-Fi for initial monitoring via an Inertial sensor LSM6DSOX at a collection rate of 100Hz. Pressure and humidity (sensor MS8607) is measured at a rate of 1Hz; the actuator is the motor shield updated every 50Hz. There are watchdog

mechanisms implemented to reset the sensors. If they read constant data for too long or stop responding, every sensor will re-initialize. While the Geiger counter continues to sample radiation pulses in the background, it updates its total micro sievert calculation and every 10 samples utilizes a Riemann sum when extracting the data.

[4.0] Preliminary Review and Predictions

[4.1] Bringing it all together

Figure 12

First, the motor housing has two D.C. motors inserted into the motor housing. Then the motor housing is placed top down in the bottom half of the shell and bonded using hot glue. Next, a lavender top

vial, containing blood, and contained inside a biohazard bag was placed inside of both circular blood slots. Next in the top half of the shell using an X-Acto knife, two parallel slits were created to hold the Geiger counter within the shell, then the Arduino and battery were glued to the side of the shell. The motor connector terminals were placed facing out of the shell to provide quick and easy access. Then the gyro sensor was placed on one of the rods facing upwards to measure the most accurate data for the z acceleration. On the top half of the shell, a switch along with two LEDs was placed to turn on the payload and feedback to know when the payload is operating. All wires were also secured to the edge of the shell to stop them from falling and getting cut or harmed by the flywheel (see [Figure 12]). Then last, the software was uploaded to Arduino.

[4.2] Blood Predictions

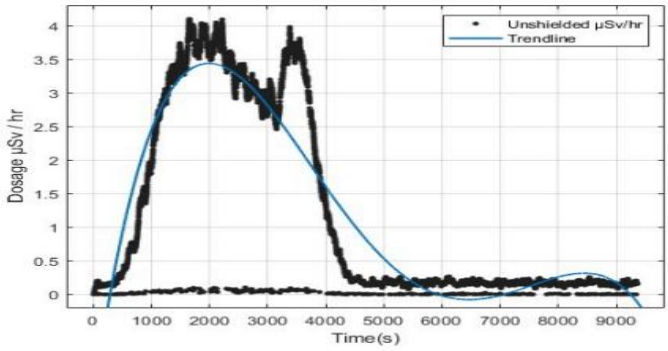

Figure 13

It is difficult to predict the changes blood will have due to the lack of extensive research on the effects of radiation on blood, and the potential for temperature to affect the composition of the blood if large gradients are felt. Taking the average data from earlier weather balloon reports provided by the National Weather Service (n.d.), the rate of ascent is around 1,000 feet (about 304.8 m) per minute and a total duration of 101 minutes. According to a recent study on radiation, (University of Colorado Boulder, Colorado Space Grant Consortium, 2025) found the total radiation dosage for an EOSS flight was around 2.5-3.0 uSv, leading to an average dosage of 3 uSv/hr (see [Figure 13]). This means on an average flight the total radiation dose is around 6uSv with adjustments for altitude and flight duration, as there is more unshielded radiation the higher the payload rises, resulting in an increased overall dosage. A Geiger counter was sent up with the payload and was expected to find a total dosage of around 5 uSv.

Human blood is typically protected from alpha and beta radiation by the shielding effect of our skin. In this experiment, the hull will be the primary barrier between the blood samples and alpha and beta radiation, significantly reducing the amount felt by beta and completely removing the potential exposure from alpha. The main radiation that will affect the blood will be gamma and neutron radiation. Gamma radiation harms all cells, including white blood cells and platelets. Neutron radiation mainly harms white blood cells, particularly lymphocytes due to their relatively large size and increased chance of neutron absorption/damage. Due to the rate of exposure, the expectation was that there would exist a small decrease in lymphocytes due to their high sensitivity but a menial change in blood count in total.

The secondary goal is to reduce mechanical damage to the blood using the shell and the gyroscope. The two points of highest mechanical risk to the blood are when the parachute is deployed, as the balloon stays in free fall and then experiences sudden deceleration as the parachute deploys. When the payload lands on the ground, wind could drag the payload, or the landing force could harm the blood. The combination of the shell and the flywheel correction system was to reduce all mechanical damage to the blood, with the expectation that there would be minimal impact on the blood as a result. During testing, the shell and the flywheel correction system prevented the blood from freezing and getting excessively cold due to the insulation provided by the shell and the heat generated by the motors.

[4.3] Gyro Review and Predictions

Figure 14

To best simulate conditions seen during flight, the flywheel correction system was tested to ensure the ability to correct unwanted rotational motion. To accomplish this test, the payload was placed between two fans and was periodically physically pushed to simulate strong and sudden winds (see [Figure 14]). The flight string was also twisted to simulate the effects of rotation caused by other payloads attached to the string. As a result of the testing, it was found that the flywheel correction system was effective at stabilization, as both passive and active correction modes provided an extremely high rate of stabilization. After testing if the correction system worked as intended, the payload was placed in a vacuum chamber alongside dry ice to test the capability of the electronics and battery system to run for extended periods of time at full load in conditions like what was expected during flight. The result of this experiment was successful, proving that the battery and electronics could run the flight time expected under extreme conditions. An additional benefit discovered during this testing was that the latent heat generated by the running of the motors maintained the internal temperature of the payload above 32 degrees F, which would assist in preventing the biological samples from freezing. This newfound benefit would additionally remove the necessity to send any heating elements up with the project, saving more mass as a result.

[4.4] Shell Review and Predictions

Impact tests, including the whip test, were performed on the payload to prove that the overall structure would not fail during moments of extreme mechanical shock. The whip test consisted of connecting the payload to a string and spinning it at high speeds. The 3-D printed bearings utilized in the project were able to withstand the force generated by the whip test and were deemed acceptable for final flight. A drop test was conducted, where the shell, and internal components, were dropped from a height

of approximately 20 feet. The payload was able to withstand the force of impact without failure and was deemed acceptable for final flight.

[5.0] Flight Day

Figure 15

On the morning of flight day, final soldering and gluing of internal components was completed, with all components being fastened securely to the internals of the hull. A pre-flight check of the motor sensors and electronics was conducted to confirm that all electrical connections were solid and that no opens in the overall circuitry existed. The flight tube was then run through the first and second bearings, where the top bearing experienced a catastrophic failure. The bottom bearing was still fully functional and capable of removing the rotation of the payload from the flight tube and attached string, and vice versa. With one bearing still intact, the project was deemed flight worthy, and preparations continued for flight. Blood was drawn immediately prior to final assembly and placed within the appropriate containment bags, which were then securely fastened into the slotted holes designed to hold the vials. The final preparation was to secure the top and bottom halves of the hull together with glue and aluminum tape. This final product was then provided to EOSS for final weighing and acceptance. The overall mass of the Sirius payload came in at ~690 g, coming in over the predicted mass and the mass budget provided by EOSS. The predicted mass of the project was ~630 g, and the team is currently investigating the cause of the remaining 60 g surplus. Thankfully, EOSS was able to accommodate the Sirius project, despite it being over the budgeted weight value.

The flight string was run along with the other payloads connecting them. Before launch the payload was held straight up and turned on for proper gyroscope calibration. While the switch for the payload main operation was pressed, the camera in the hull was, in error, not turned on. Then the balloon launched along with the Sirius payload (see [Figure 15]). The payload experienced a rapid accent and decent, but upon recovery, it was found that the flight tube was ripped out of the project itself, causing an internal failure of the motor housing. It was estimated, by EOSS, that when the payload touched down on Earth, the knot made at the bottom of the flight tube to secure the flight string to the flight tube was not large enough, causing the flight string to separate from the tube and allow free movement of the Sirius project on the string (see [Figure 16]). The resulting crash and instability caused additional damage to the payload when being dragged along the field in which the payloads were recovered.

Figure 16

[6.0] Conclusion

[6.1] Blood

Once the blood testing was completed and the data from the SD card was recovered, there were some intriguing results. One problem occurred because there were so few white blood cells left in the post flight sample that there could be no measurement of lymphocytes. in the data between pre(control) and post(test) it was found that a general cell count decrease did happen, but it was most drastic with the white blood cells . The first conclusion drawn was that a combination of both radiation exposure, temperature changes, and pressure changes caused the sharp decrease in white blood cell count in the final sample. To test this conclusion, the Sirius team conducted two quick tests with six freshly drawn blood samples from the same two donors that gave samples for the first set of tests. One of the two new tests conducted included utilizing a pressure chamber to expose two blood samples to the same overall pressure changes experienced during flight brake (see [30, Sec. 8.3.1]).. The second of the two new tests conducted included utilizing known radioactive sources, Co-60 for gamma and Sr-90 for beta, to irradiate two blood samples to the same overall exposure that was experienced during the flight, checked against the data retrieved from the onboard Geiger counter (see [Figure 17]).

Two control samples were used to test against these four samples to provide a baseline for damage as a result of these new tests. The results showed no white blood cell death because of either the radioactive exposure or overall pressure changes. The remaining factor that could have caused the damage seen from the results of the original experiment was identified as mechanical shock. When the balloon that carries the Demosat projects pops at ~100,000 feet, a parachute is utilized to prevent all of the projects from falling down to Earth at terminal velocity. This parachute, however, does not immediately deploy upon the popping of the balloon. There exists a delay between the two events, which allows for a drastic acceleration of the group of projects towards the surface of the Earth. When the parachute does deploy, the resulting shock to the individual systems simulates that of a whipping motion, where all the projects and the individual components inside experience a force that is a factor of magnitude greater than Earth’s gravitational pull. A second mechanical shock is experienced upon the landing of the string of Demosat projects at the final point of descent. The sum of both shocks has been identified as the cause of the white blood cell damage seen from the original test.

The theory as to why the mechanical shock caused the mass white cell death is due to the large relative size of the white blood cells compared to that of the red blood cells. The red blood cell count did experience a small degradation between the two samples but did not show as large of a decrease as that of the white blood cells. This is potentially due to the overall shock experienced by these white blood cells compared to that of the red blood cells. To draw a more final conclusion as to the reason why the white

blood cells experienced a higher rate of degradation, a whip and drop test with the blood vials is necessary.

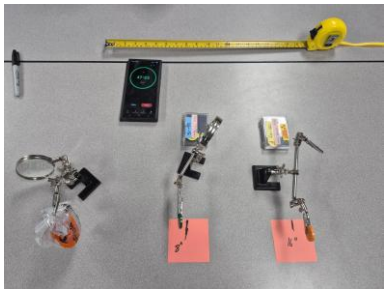

Figure 17

Figure 18

The Sirius team concludes that the blood was weakened and subsequently damaged by the two mechanical shocks experienced during the flight. There was no conclusion that the radioactive exposure experienced during the flight, or the pressure and temperature changes experienced caused any cell damage to the blood, as verified by the two independent tests conducted after the original testing was concluded.

[6.2] Flywheel System and Payload Design

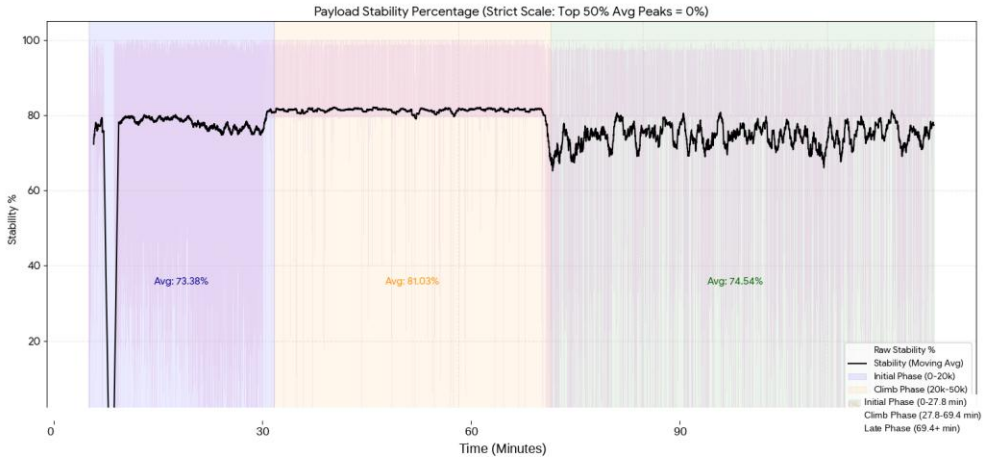

Figure 19

A comparison can be drawn from the data collected by the Sirius project to the last documented attempted by a team from CSU to stabilize a payload. (See. [3, Sec. 2.2]) In CSU's previous attempt achieved 54% percent stabilization when their stabilization system was active. (University of Colorado Boulder, Colorado Space Grant Consortium (2023))

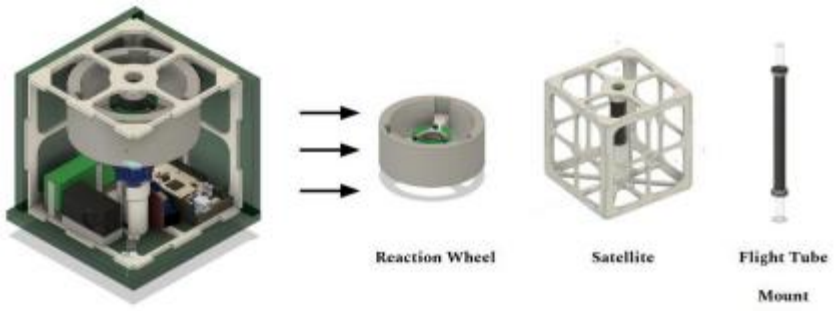

Figure 20

CSU had attempted a correction system by utilizing a reaction wheel, while utilizing a cube shape as the shape of their payload (see [Figure 20]). The box shape this likely made correction more difficult due to the added leverage the wind could gain against their payload. An additional reason for the difference between the two stabilization data sets between the two projects may be due to the one-wheel design versus two-wheel design utilized (see [7, Sec 3.3.1]).

The Sirius team also approximated the stabilization percentage using the formula below:

$$S = \left(1 - \frac{\sum |\theta_a - \theta_t|}{n \cdot \theta_{max}}\right) \times 100$$

The resulting stabilization percentage from this equation showed that the Sirius team was able to achieve an approximate 73% stabilization level utilizing only the overall design of the hull with neither of the correction systems operating. Despite this high level of stabilization, there still exists a high amount of rotation when exposed to high wind speeds at altitude. This can be seen by an average acceleration of 8.60 $\pm$ 0.04 [deg/s^2]. A max speed of 629.1 $\pm$ 0.04 [deg/s] indicated that the shell itself failed to address extremely high rotational forces. In conclusion, the shell manages to heighten stabilization but fails to address strong angular forces. The next phase of flight had an active correction system in use. The data recorded from this leg of the flight showed a correction percentage of approximately 81%. Additionally, an average decrease in acceleration of 5.18 [deg/s] was recorded, with a maximum rotational speed of 129.18 $\pm$ 0.04 being logged (see [Figure 19]). These new datasets indicate that the flywheel correction system both improves overall general stability and decreases the maximum rotational speed experienced by the payload. The last phase of flight had the passive correction system in use. The data recorded from this correction system showed a stabilization percentage of approximately 75%. This data proves that both the active and passive corrections systems improved general stability and reduced the speed of rotation by a significant amount.

After the test flight had occurred, the entire Sirius project was rebuilt in CAD software for the purpose of measuring the moment of inertia of the project. The CAD software results gave a moment of inertia for the entire payload as 1.56E-3 kg*m^2, while the flywheel system was measured to have a moment of inertia of 3.00E-4 kg*m^2. As seen in these results, the payload had a moment of inertia that was approximately 5 times greater than that of the flywheel system. This relatively small difference in moment of inertia was beneficial in the overall performance of the payload, as the rotation of the payload, and resulting momentum, would be absorbed by the internal flywheel system when the wheels were spun up in

the opposite direction. This was one of the key reasons why the system could maintain a high level of stabilization.

Overall, the design of the hull reduced overall angular acceleration and was able to provide an average of 73% stabilization percentage. The active and passive flywheel systems were able to build and improve upon this stabilization, achieving 81% and 75% stabilization, respectively.

[6.3] Other Data and Correlations

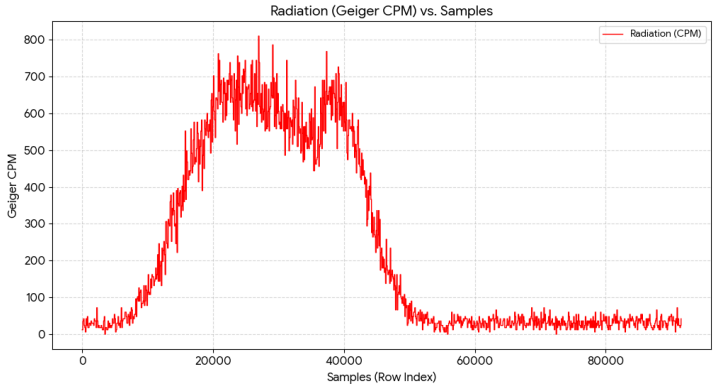

Figure 21

There was a total radiation dosage of 3.52 uSv ± .7uSv. This graph (see [Figure 21]) is almost identical to the last study on radiation conducted by a previous FRCC team (University of Colorado Boulder, Colorado Space Grant Consortium (2025)).

Using the manufacturer specifications for the parachute and total volume captured by the parachute provided by EOSS, found that at most the payload experienced 1-2 G's maximum when the balloon popped at roughly 85,000 ft. It free falls at 106 ft/s because there is such little air density that there's nothing for the parachute to grab, which could cause a sudden jerk (see [Figure 22]). At about 6,000 ft at only 18 ft/s (12.3 mph) the payload came to a sudden stop and impacted the ground. On impact, the payload experienced 10.6 G’s of deceleration. Because the individual pressure and radiation controls returned from flight with no detectable damage, the observed biological trauma was isolated to the ground impact. While radiation and pressure may have been contributors, we expect the primary cause to be terminal impact.

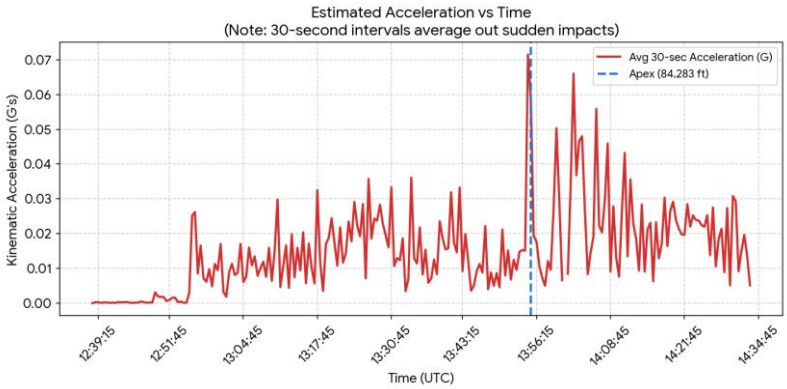

Figure 22

[7.0] Reflection

The Sirius team worked diligently over the course of this project, combining a myriad of different skillsets and knowledge to achieve the stated goals and test completions. The original goals of this project were lofty, with many recommendations to pare down the experiments and simplify the engineering design. The team remained steadfast in their endeavors, pushing forward with the idea of combining biological experimentation with engineering stabilization and structural design. While the scope of the tests for the blood had to be scaled down from the first iteration due to a lack of budget, the overall spirit of the biological tests remained, comparing the effects of changing radiation exposure rates at differing altitudes on the overall count of different cells in the samples. The engineering side of this project proved to be a monumental task, requiring extensive knowledge of Arduino coding, materials science, physics, and electrical circuitry and design.

The flywheel stabilization setup was continuously changed throughout the design process, ranging from different angles in which the flywheels were aligned to provide an internal torque on different axes, to the design of the structural support in which the flywheels and motors were mounted. In the end, the team landed on the current version of the Sirius experiment, providing the maximum amount of rotational stability, biological testing capability, and mass efficiency in one package. Despite the successes of this project, the team acknowledges that many areas of these experiments can be greatly improved to provide better results and more reliable scientific data. The entire team grew because of this comprehensive design process, with many members learning new skills and reinforcing previous knowledge.

[7.1] Future iterations and studies

The Sirius project team recommends that these experiments be performed again; to verify and expand upon the results seen from the Sirius payload. It is recommended that future studies are conducted with higher sample sizes to further validate the results of the Sirius project's performed studies. Recommendations for future iterations include bolstering the 3-D printed bearings that separated the payload from the other projects included on the flight string, as the Sirius team experienced a full breakdown of the top baring before flight. Ensuring that these bearings remain intact and stable throughout the flight guarantees that the rotation data measured by the onboard accelerometer does not include rotation due to twisting of the string from the rotation of other projects during flight.

The Sirius team recommends that a future project be designed and tested to minimize the mechanical shock experienced during flight. The ability to cushion the biological samples during the parachute deployment and final touchdown would be an exciting development, as it would allow for a similar test to the Sirius project to be conducted with the removal of damage caused by mechanical shock. This would allow for the biological samples to be tested and have any damage isolated to the effects of radioactive exposure and temperature/pressure changes experienced during flight.

The team also recommends that an “air-brake” be added to the bottom of the payload, as the overall design of the Sirius project, being very aerodynamic and intended to reduce drag force from the wind, aided in the acceleration of the project upon the balloon popping, which may have contributed to the failure of the bottom bearing when the parachute deployed and a large resulting force was applied to the Sirius payload. An “air-brake” designed in a way that would allow for rotational force due to the wind to be mitigated but allowing for a drag force to be felt during free-fall would be beneficial to the overall health of the payload during its descent.

[8.0] Appendices

[8.1] General

[8.1.1] Cost and supply list

Parts	Quantity	Cost	Supplier
Data Logging shield	1	$13.95	Adafruit
Motor/Stepper/Servo Shield	1	$19.95	Adafruit
Accelerometer and Gyroscope	1	$11.95	Adafruit
Pressure Humidity Temperature	1	$14.95	Adafruit
Geiger Counter	1	$99.95	Adafruit
22AWG Solid Core wire	1	$15.95	Adafruit
Micro Servo	1	$5.95	Adafruit
STEMMA QT / Qwiic to pin	2	$0.95	Adafruit
STEMMA QT / Qwiic double end	2	$1.25	Adafruit
STEMMA JST PH 2mm 3-Pin	1	$1.25	Adafruit
JST PH 2mm 3-pin	1	$0.75	Adafruit
Arduino UNO Q	1	$44.00	Arduino
UV Detection Stickers	1	$16.49	Amazon
DC Motor	2	$6.49	Amazon
Standalone camera	1	$69.99	Amazon
Chemical heat pack	1	$24.99	Amazon
LED kit	1	$11.99	Amazon
Resistor kit	1	$9.99	Amazon
64 GB SD card	1	$14.94	Amazon
Cr1220 battery	1	$5.99	Amazon
Hyper PLA-CF	1	$24.64	Amazon
Hand warmers	1	$6.99	Amazon
		$423.35	

[8.2] Blood Test Forms

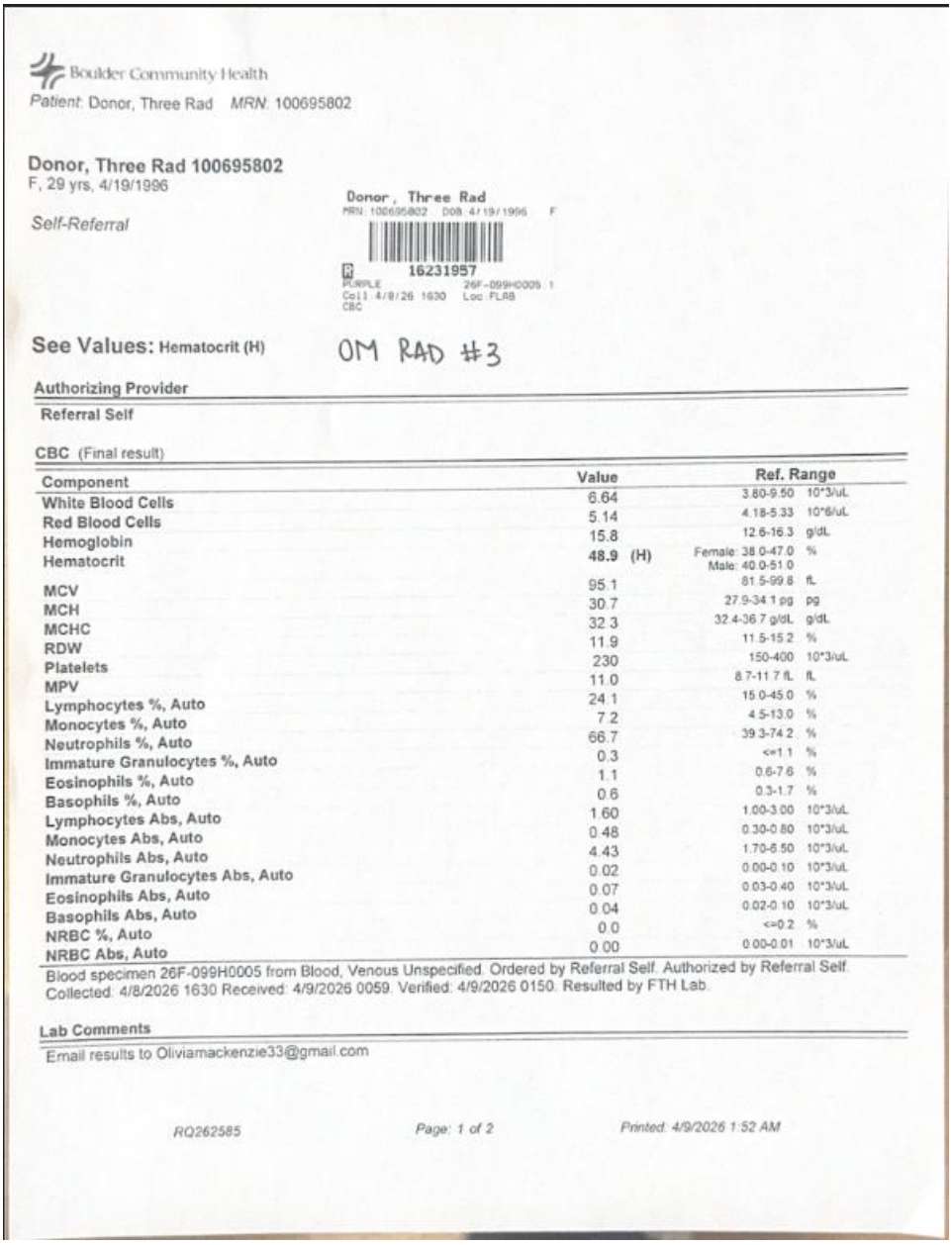

Boulder Community Health

Patient: Donor, Three Rad MRN: 100695802

Donor, Three Rad 100695802
F, 29 yrs, 4/19/1996

Self-Referral

Donor, Three Rad
MRN: 100695802 DOB: 4/19/1996 F
16231957
PURPLE 26F-099H0005.1
Coll: 4/8/26 1630 Loc: FLAB
CBC

See Values: Hematocrit (H) OM RAD #3

Authorizing Provider

Referral Self

CBC (Final result)

Component	Value		Ref. Range	
White Blood Cells	6.64		3.80-9.50	10*3/uL
Red Blood Cells	5.14		4.18-5.33	10*6/uL
Hemoglobin	15.8		12.6-16.3	g/dL
Hematocrit	48.9	(H)	Female: 38.0-47.0 Male: 40.0-51.0	%
MCV	95.1		81.5-99.8	fL
MCH	30.7		27.9-34.1 pg	pg
MCHC	32.3		32.4-36.7 g/dL	g/dL
RDW	11.9		11.5-15.2	%
Platelets	230		150-400	10*3/uL
MPV	11.0		8.7-11.7 fL	fL
Lymphocytes %, Auto	24.1		15.0-45.0	%
Monocytes %, Auto	7.2		4.5-13.0	%
Neutrophils %, Auto	66.7		39.3-74.2	%
Immature Granulocytes %, Auto	0.3		<=1.1	%
Eosinophils %, Auto	1.1		0.6-7.6	%
Basophils %, Auto	0.6		0.3-1.7	%
Lymphocytes Abs, Auto	1.60		1.00-3.00	10*3/uL
Monocytes Abs, Auto	0.48		0.30-0.80	10*3/uL
Neutrophils Abs, Auto	4.43		1.70-6.50	10*3/uL
Immature Granulocytes Abs, Auto	0.02		0.00-0.10	10*3/uL
Eosinophils Abs, Auto	0.07		0.03-0.40	10*3/uL
Basophils Abs, Auto	0.04		0.02-0.10	10*3/uL
NRBC %, Auto	0.0		<=0.2	%
NRBC Abs, Auto	0.00		0.00-0.01	10*3/uL

Blood specimen 26F-099H0005 from Blood, Venous Unspecified. Ordered by Referral Self. Authorized by Referral Self. Collected: 4/8/2026 1630 Received: 4/9/2026 0059. Verified: 4/9/2026 0150. Resulted by FTH Lab.

Lab Comments

Email results to Oliviamackenzie33@gmail.com

RQ262585 Page: 1 of 2 Printed: 4/9/2026 1:52 AM

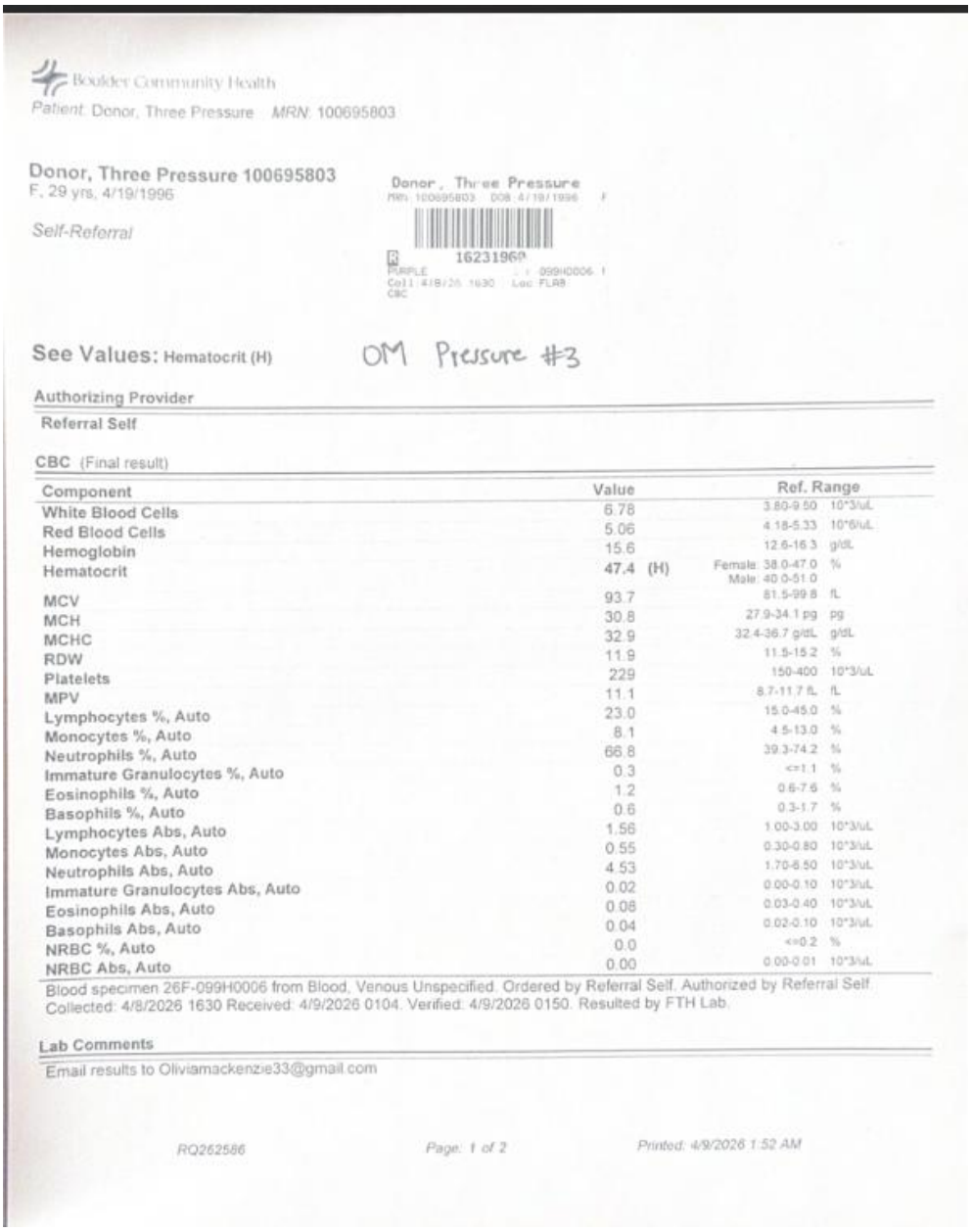

Boulder Community Health

Patient: Donor, Three Pressure MRN: 100695803

Donor, Three Pressure 100695803
F, 29 yrs, 4/19/1996

Self-Referral

Donor, Three Pressure
MRN: 100695803 DOB: 4/19/1996 F
16231960
PURPLE 099H0006 1
Coll: 4/8/26 1630 Loc: FLAB
CBC

See Values: Hematocrit (H) OM Pressure #3

Authorizing Provider
Referral Self

CBC (Final result)

Component	Value	Ref. Range
White Blood Cells	6.78	3.80-9.50 10*3/uL
Red Blood Cells	5.06	4.18-5.33 10*6/uL
Hemoglobin	15.6	12.6-16.3 g/dL
Hematocrit	47.4 (H)	Female: 38.0-47.0 % Male: 40.0-51.0
MCV	93.7	81.5-99.8 fL
MCH	30.8	27.9-34.1 pg pg
MCHC	32.9	32.4-36.7 g/dL g/dL
RDW	11.9	11.5-15.2 %
Platelets	229	150-400 10*3/uL
MPV	11.1	8.7-11.7 fL fL
Lymphocytes %, Auto	23.0	15.0-45.0 %
Monocytes %, Auto	8.1	4.5-13.0 %
Neutrophils %, Auto	66.8	39.3-74.2 %
Immature Granulocytes %, Auto	0.3	<=1.1 %
Eosinophils %, Auto	1.2	0.6-7.6 %
Basophils %, Auto	0.6	0.3-1.7 %
Lymphocytes Abs, Auto	1.56	1.00-3.00 10*3/uL
Monocytes Abs, Auto	0.55	0.30-0.80 10*3/uL
Neutrophils Abs, Auto	4.53	1.70-6.50 10*3/uL
Immature Granulocytes Abs, Auto	0.02	0.00-0.10 10*3/uL
Eosinophils Abs, Auto	0.08	0.03-0.40 10*3/uL
Basophils Abs, Auto	0.04	0.02-0.10 10*3/uL
NRBC %, Auto	0.0	<=0.2 %
NRBC Abs, Auto	0.00	0.00-0.01 10*3/uL

Blood specimen 26F-099H0006 from Blood, Venous Unspecified. Ordered by Referral Self. Authorized by Referral Self. Collected: 4/8/2026 1630 Received: 4/9/2026 0104. Verified: 4/9/2026 0150. Resulted by FTH Lab.

Lab Comments
Email results to Oliviamackenzie33@gmail.com

RQ262586 Page: 1 of 2 Printed: 4/9/2026 1:52 AM

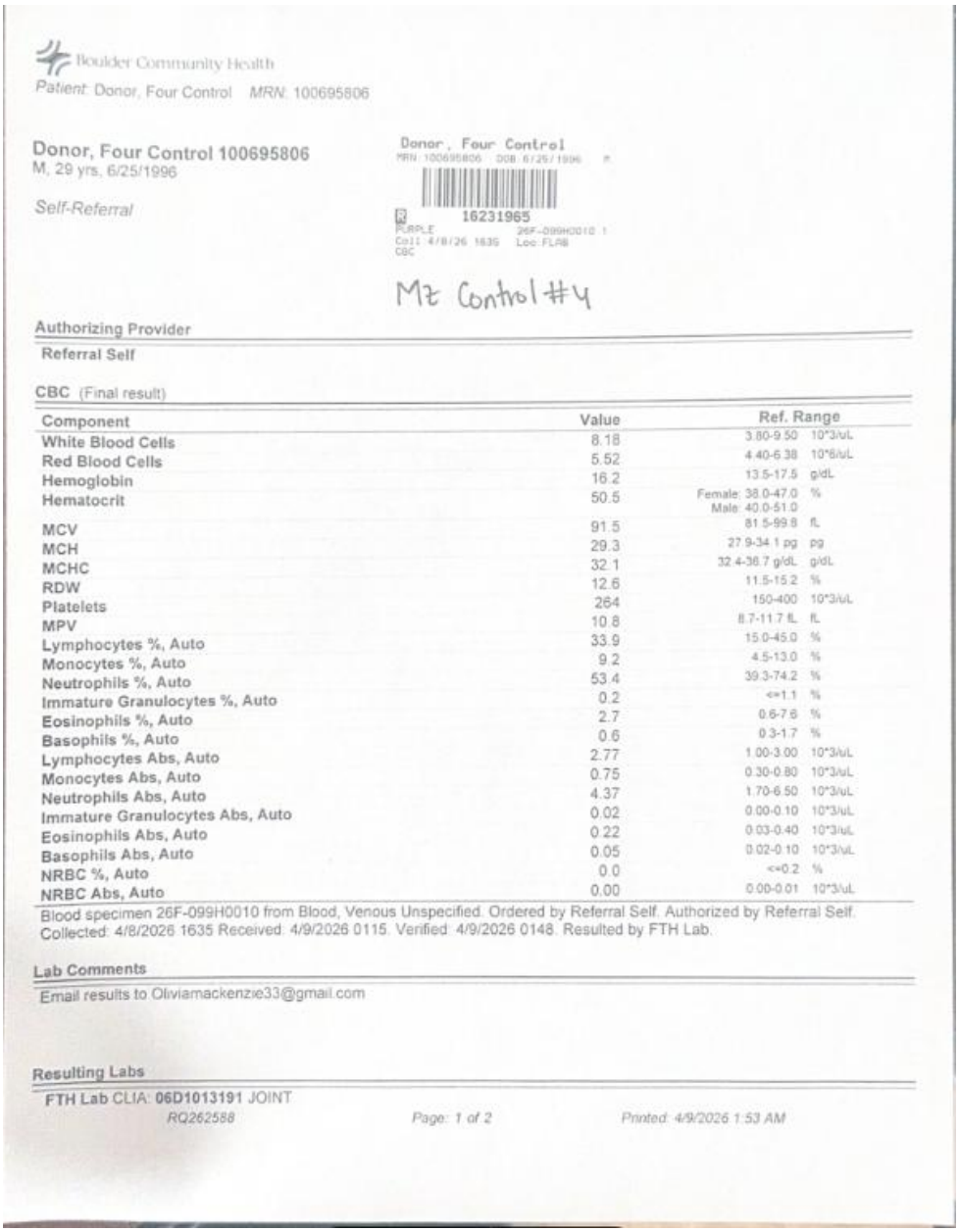

Boulder Community Health

Patient: Donor, Four Control MRN: 100695806

Donor, Four Control 100695806
M, 29 yrs, 6/25/1996

Self-Referral

Donor, Four Control
MRN: 100695806 DOB: 6/25/1996 F
16231965
PURPLE 26F-099H0010.1
Coll: 4/8/26 1635 Loc: FLAB
CBC

Mt Control #4

Authorizing Provider

Referral Self

CBC (Final result)

Component	Value	Ref. Range
White Blood Cells	8.18	3.80-9.50 10*3/uL
Red Blood Cells	5.52	4.40-6.38 10*6/uL
Hemoglobin	16.2	13.5-17.5 g/dL
Hematocrit	50.5	Female: 38.0-47.0 % Male: 40.0-51.0
MCV	91.5	81.5-99.8 fL
MCH	29.3	27.9-34.1 pg pg
MCHC	32.1	32.4-36.7 g/dL g/dL
RDW	12.6	11.5-15.2 %
Platelets	264	150-400 10*3/uL
MPV	10.8	8.7-11.7 fL fL
Lymphocytes %, Auto	33.9	15.0-45.0 %
Monocytes %, Auto	9.2	4.5-13.0 %
Neutrophils %, Auto	53.4	39.3-74.2 %
Immature Granulocytes %, Auto	0.2	<=1.1 %
Eosinophils %, Auto	2.7	0.6-7.6 %
Basophils %, Auto	0.6	0.3-1.7 %
Lymphocytes Abs, Auto	2.77	1.00-3.00 10*3/uL
Monocytes Abs, Auto	0.75	0.30-0.80 10*3/uL
Neutrophils Abs, Auto	4.37	1.70-6.50 10*3/uL
Immature Granulocytes Abs, Auto	0.02	0.00-0.10 10*3/uL
Eosinophils Abs, Auto	0.22	0.03-0.40 10*3/uL
Basophils Abs, Auto	0.05	0.02-0.10 10*3/uL
NRBC %, Auto	0.0	<=0.2 %
NRBC Abs, Auto	0.00	0.00-0.01 10*3/uL

Blood specimen 26F-099H0010 from Blood, Venous Unspecified. Ordered by Referral Self. Authorized by Referral Self. Collected: 4/8/2026 1635 Received: 4/9/2026 0115. Verified: 4/9/2026 0148. Resulted by FTH Lab.

Lab Comments

Email results to Oliviamackenzie33@gmail.com

Resulting Labs

FTH Lab CLIA: **06D1013191** JOINT

RQ262588 *Page: 1 of 2* *Printed: 4/9/2026 1:53 AM*

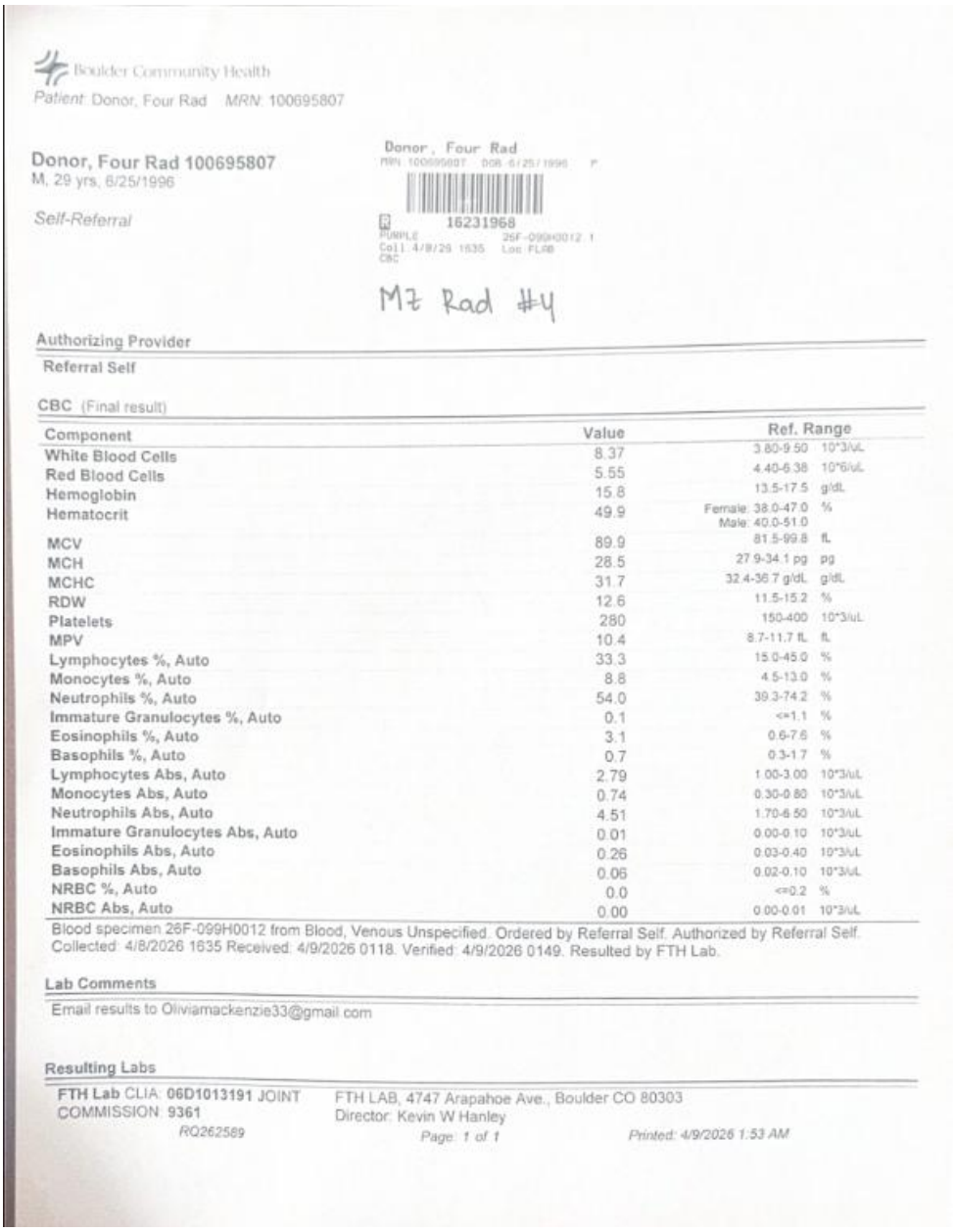

Boulder Community Health

Patient: Donor, Four Rad MRN: 100695807

Donor, Four Rad 100695807
M, 29 yrs, 6/25/1996

Self-Referral

Donor , Four Rad
MRN: 100695807 DOB: 6/25/1996 F
16231968
PURPLE 26F-099H0012 1
Coll: 4/8/26 1635 Loc: FLAB
CBC

M7 Rad #4

Authorizing Provider

Referral Self

CBC (Final result)

Component	Value	Ref. Range
White Blood Cells	8.37	3.80-9.50 10*3/uL
Red Blood Cells	5.55	4.40-6.38 10*6/uL
Hemoglobin	15.8	13.5-17.5 g/dL
Hematocrit	49.9	Female: 38.0-47.0 % Male: 40.0-51.0
MCV	89.9	81.5-99.8 fL
MCH	28.5	27.9-34.1 pg pg
MCHC	31.7	32.4-36.7 g/dL g/dL
RDW	12.6	11.5-15.2 %
Platelets	280	150-400 10*3/uL
MPV	10.4	8.7-11.7 fL fL
Lymphocytes %, Auto	33.3	15.0-45.0 %
Monocytes %, Auto	8.8	4.5-13.0 %
Neutrophils %, Auto	54.0	39.3-74.2 %
Immature Granulocytes %, Auto	0.1	<=1.1 %
Eosinophils %, Auto	3.1	0.6-7.6 %
Basophils %, Auto	0.7	0.3-1.7 %
Lymphocytes Abs, Auto	2.79	1.00-3.00 10*3/uL
Monocytes Abs, Auto	0.74	0.30-0.80 10*3/uL
Neutrophils Abs, Auto	4.51	1.70-6.50 10*3/uL
Immature Granulocytes Abs, Auto	0.01	0.00-0.10 10*3/uL
Eosinophils Abs, Auto	0.26	0.03-0.40 10*3/uL
Basophils Abs, Auto	0.06	0.02-0.10 10*3/uL
NRBC %, Auto	0.0	<=0.2 %
NRBC Abs, Auto	0.00	0.00-0.01 10*3/uL

Blood specimen 26F-099H0012 from Blood, Venous Unspecified. Ordered by Referral Self. Authorized by Referral Self. Collected: 4/8/2026 1635 Received: 4/9/2026 0118. Verified: 4/9/2026 0149. Resulted by FTH Lab.

Lab Comments

Email results to Oliviamackenzie33@gmail.com

Resulting Labs

FTH Lab CLIA: **06D1013191** JOINT COMMISSION: **9361**
RQ262589

FTH LAB, 4747 Arapahoe Ave., Boulder CO 80303
Director: Kevin W Hanley

Page: 1 of 1 *Printed: 4/9/2026 1:53 AM*

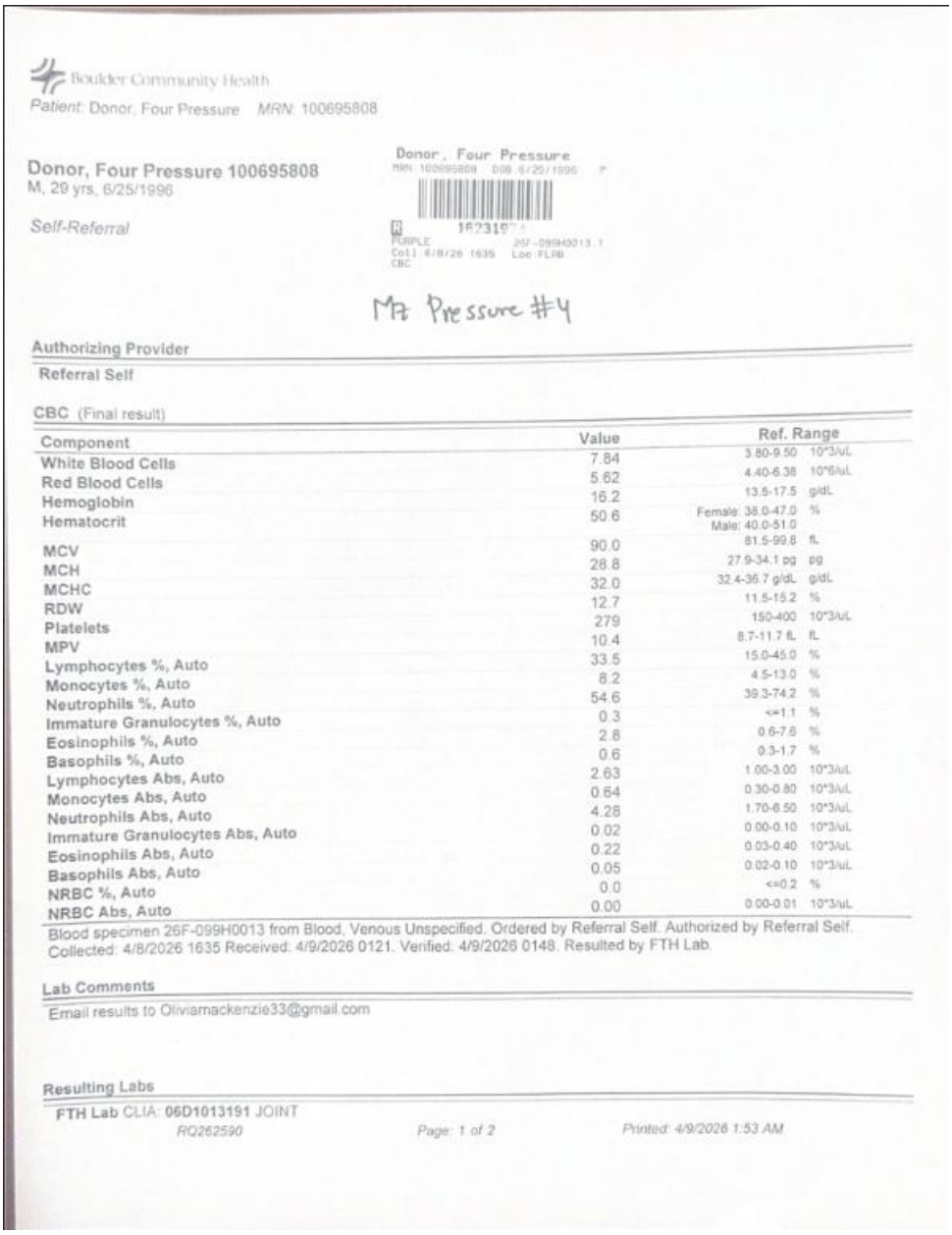

Boulder Community Health

Patient: Donor, Four Pressure *MRN:* 100695808

Donor, Four Pressure 100695808
M, 29 yrs, 6/25/1996

Self-Referral

Donor, Four Pressure
MRN: 100695808 DOB: 6/25/1996 F
162319
PURPLE 26F-099H0013.1
Coll: 4/8/26 1635 Loc: FLAB
CBC

M7 Pressure #4

Authorizing Provider

Referral Self

CBC (Final result)

Component	Value	Ref. Range
White Blood Cells	7.84	3.80-9.50 10*3/uL
Red Blood Cells	5.62	4.40-6.36 10*6/uL
Hemoglobin	16.2	13.5-17.5 g/dL
Hematocrit	50.6	Female: 38.0-47.0 % Male: 40.0-51.0
MCV	90.0	81.5-99.8 fL
MCH	28.8	27.9-34.1 pg pg
MCHC	32.0	32.4-36.7 g/dL g/dL
RDW	12.7	11.5-15.2 %
Platelets	279	150-400 10*3/uL
MPV	10.4	8.7-11.7 fL fL
Lymphocytes %, Auto	33.5	15.0-45.0 %
Monocytes %, Auto	8.2	4.5-13.0 %
Neutrophils %, Auto	54.6	39.3-74.2 %
Immature Granulocytes %, Auto	0.3	<=1.1 %
Eosinophils %, Auto	2.8	0.6-7.6 %
Basophils %, Auto	0.6	0.3-1.7 %
Lymphocytes Abs, Auto	2.63	1.00-3.00 10*3/uL
Monocytes Abs, Auto	0.64	0.30-0.80 10*3/uL
Neutrophils Abs, Auto	4.28	1.70-6.50 10*3/uL
Immature Granulocytes Abs, Auto	0.02	0.00-0.10 10*3/uL
Eosinophils Abs, Auto	0.22	0.03-0.40 10*3/uL
Basophils Abs, Auto	0.05	0.02-0.10 10*3/uL
NRBC %, Auto	0.0	<=0.2 %
NRBC Abs, Auto	0.00	0.00-0.01 10*3/uL

Blood specimen 26F-099H0013 from Blood, Venous Unspecified. Ordered by Referral Self. Authorized by Referral Self. Collected: 4/8/2026 1635 Received: 4/9/2026 0121. Verified: 4/9/2026 0148. Resulted by FTH Lab.

Lab Comments

Email results to Oliviamackenzie33@gmail.com

Resulting Labs

FTH Lab CLIA: **06D1013191** JOINT
RQ262590 *Page: 1 of 2* *Printed: 4/9/2026 1:53 AM*

Boulder Community Health
Patient: [redacted] MRN:

Post, Donor Tue
MRN: U DOB: U U

Self-Referral

Final Report

See Values: RDW (H)

Authorizing Provider

Doctor Not On File	F: 000-000-0000

CBC (Final result)

Component	Value	Ref. Range	
White Blood Cells	4.85	4.18 - 6.38	10*6/uL
Red Blood Cells	16.7	13.5 - 17.5	g/dL
Hemoglobin	47.0	Female: 38.0-47.0 Male: 40.0-51.0	%
Hematocrit	96.9	81.5 - 99.8	fL
MCV	34.4	27.9-34.1 pg	pg
MCH	35.5	32.4-36.7 g/dL	g/dL
MCHC	**21.2 (H)**	11.5 - 15.2	%
RDW	191	150 - 400	10*3/uL
Platelets	12.3	8.7-11.7 fL	fL
MPV			

Blood specimen 26F-094H0163 from Blood, Venous Unspecified. Ordered by Doctor Not On File. Authorized by Doctor Not On File. Collected: 4/4/2026 0500 Received: 1252. Verified: 4/4/2026 1323. Resulted by FTH Lab.

Canceled Tests

Pathologist Review Reason: zOther - Research sample, not required.
Peripheral Blood Smear Reason: zOther - Research sample, not required.
Platelet Estimate Reason: zOther - Research sample, not required.

Resulting Labs

FTH Lab CLIA: **06D1013191** JOINT COMMISSION: **9361**	FTH LAB, 4747 Arapahoe Ave., Boulder CO 80303 Director: Kevin W Hanley

Legend

H - High

RQ262241 *Page: 1 of 1* *Printed: 4/4/2026 2:02 PM*

Boulder Community Health

Patient: [redacted] *MRN:*

Pre, Donor Two
MRN: U DOB: U U

Self-Referral

Final Report

See Values: **White Blood Cells (H), Hematocrit (H), Lymphocytes Abs, Auto (H), Monocytes Abs, Auto (H), Eosinophils Abs, Auto (H)**

Authorizing Provider

Doctor Not On File F: 000-000-0000

CBC (Final result)

Component	Value		Ref. Range	
White Blood Cells	11.08	(H)	3.60 - 9.50	10*3/uL
Red Blood Cells	5.71		4.18 - 6.38	10*6/uL
Hemoglobin	16.5		13.5 - 17.5	g/dL
Hematocrit	52.9	(H)	Female: 38.0-47.0 Male: 40.0-51.0	%
MCV	92.6		81.5 - 99.8	fL
MCH	28.9		27.9-34.1 pg	pg
MCHC	31.2		32.4-36.7 g/dL	g/dL
RDW	13.1		11.5 - 15.2	%
Platelets	271		150 - 400	10*3/uL
MPV	10.8		8.7-11.7 fL	fL
Lymphocytes %, Auto	37.2		15.0 - 45.0	%
Monocytes %, Auto	9.5		4.5 - 13.0	%
Neutrophils %, Auto	48.2		39.3 - 74.2	%
Immature Granulocytes %, Auto	0.3		<=1.1	%
Eosinophils %, Auto	4.3		0.6 - 7.6	%
Basophils %, Auto	0.5		0.3 - 1.7	%
Lymphocytes Abs, Auto	4.12	(H)	1.00 - 3.00	10*3/uL
Monocytes Abs, Auto	1.05	(H)	0.30 - 0.80	10*3/uL
Neutrophils Abs, Auto	5.35		1.70 - 6.50	10*3/uL
Immature Granulocytes Abs, Auto	0.03		0.00 - 0.10	10*3/uL
Eosinophils Abs, Auto	0.48	(H)	0.03 - 0.40	10*3/uL
Basophils Abs, Auto	0.05		0.02 - 0.10	10*3/uL
NRBC %, Auto	0.0		<=0.2	%
NRBC Abs, Auto	0.00		0.00 - 0.01	10*3/uL

Blood specimen 26F-094H0162 from Blood, Venous Unspecified. Ordered by Doctor Not On File. Authorized by Doctor Not On File. Collected: 4/4/2026 0500 Received: 1248. Verified: 4/4/2026 1308. Resulted by FTH Lab.

Resulting Labs

FTH Lab CLIA: **06D1013191** JOINT COMMISSION: **9361**
FTH LAB, 4747 Arapahoe Ave., Boulder CO 80303
Director: Kevin W Hanley

RQ262240 *Page: 1 of 2* *Printed: 4/4/2026 2:01 PM*

Boulder Community Health

Patient: [redacted] *MRN:*

Pre, Donor One
MRN: U DOB: U U

Self-Referral

Final Report

See Values: White Blood Cells (H), RDW (H)

Authorizing Provider

Doctor Not On File F: 000-000-0000

CBC (Final result)

Component	Value	Ref. Range
White Blood Cells	**9.61 (H)**	3.80 - 9.50 10*3/uL
Red Blood Cells	5.34	4.18 - 6.38 10*6/uL
Hemoglobin	14.9	13.5 - 17.5 g/dL
Hematocrit	47.6	Female: 38.0-47.0 % Male: 40.0-51.0
MCV	89.1	81.5 - 99.8 fL
MCH	27.9	27.9-34.1 pg pg
MCHC	31.3	32.4-36.7 g/dL g/dL
RDW	**35.5 (H)**	11.5 - 15.2 %
Platelets	157	150 - 400 10*3/uL

Blood specimen 26F-094H0165 from Blood, Venous Unspecified. Ordered by Doctor Not On File. Authorized by Doctor Not On File. Collected: 4/4/2026 0430 Received: 1258. Verified: 4/4/2026 1323. Resulted by FTH Lab.

Canceled Tests

Manual Differential Reason: zOther - Research samples, no differential required
Peripheral Blood Smear Reason: zOther - Research sample, not required.
Platelet Estimate Reason: zOther - Research sample, not required.

Resulting Labs

FTH Lab CLIA: **06D1013191** JOINT COMMISSION: **9361**
FTH LAB, 4747 Arapahoe Ave., Boulder CO 80303
Director: Kevin W Hanley

Legend

H - High

RQ262242 *Page: 1 of 1* *Printed: 4/4/2026 2:00 PM*

Boulder Community Health
Patient: [redacted] MRN:

Post, Donor One
MRN: U DOB: U U

Self-Referral

Final Report

See Values: White Blood Cells (LL), RDW (H), Platelets (L)

Authorizing Provider

Doctor Not On File F: 000-000-0000

CBC (Final result)

Component	Value	Ref. Range
White Blood Cells	0.76 (LL)	3.80 - 9.50 10*3/uL
Red Blood Cells	4.54	4.18 - 6.38 10*6/uL
Hemoglobin	14.4	13.5 - 17.5 g/dL
Hematocrit	42.8	Female: 38.0-47.0 % Male: 40.0-51.0
MCV	94.3	81.5 - 99.8 fL
MCH	31.7	27.9-34.1 pg pg
MCHC	33.6	32.4-36.7 g/dL g/dL
RDW	21.1 (H)	11.5 - 15.2 %
Platelets	41 (L)	150 - 400 10*3/uL
MPV	12.7	8.7-11.7 fL fL

Blood specimen 26F-094H0166 from Blood, Venous Unspecified. Ordered by Doctor Not On File. Authorized by Doctor Not On File. Collected: 4/4/2026 0430 Received: 1300. Verified: 4/4/2026 1330. Resulted by FTH Lab.

Canceled Tests

Manual Differential Reason: zOther - Research samples, no differential required
Pathologist Review Reason: zOther - Research sample, not required.
Peripheral Blood Smear Reason: zOther - Research sample, not required.
Platelet Estimate Reason: zOther - Research sample, not required.

Resulting Labs

FTH Lab CLIA: **06D1013191** JOINT COMMISSION: **9361**
FTH LAB, 4747 Arapahoe Ave., Boulder CO 80303
Director: Kevin W Hanley

Legend

L - Low **H** - High **LL** - Low Panic

Communication Logs

CBC 26F-094H0166

RQ262243 *Page: 1 of 2* *Printed: 4/4/2026 1:45 PM*

[8.3] Data Samples, and Extra Graphs

Total average for flight:	Standard diviation	Average before stablization inticilazation	Max and min beforce stablization incilization
Average gryro Z(deg)	Gyro Z (deg)	Average gyro Z(deg)	Max GyroZ (deg)
19.4	68.7	100.6	227.10
Average Accel Z(deg)	Accel Z (deg)	Average Accel Z(deg)	min gyroIZ (deg)
5.018	12.043	8.60	0
Average Temp(c)	Temp (c)	Average Passive stablization	Max and min after passive stablization incilization
-1.05	0.169	Average gyro Z(deg)	Max gyroZ (deg)
NOTE temp, pressure and humdity failed after 120second of data	Pressure (Pa)	11.2	145.07
Average Pressure(Pa)	31305	Average Accel Z(deg)	min gyroZ (deg)
20369	Giger Cpm	5.40	0
Average radiation dose per second (uSv/s)	259.55	Average Active stablization	Max and min after active stablization incilization
0.000	uSv	Average gyro Z(deg)	Max gyroZ (deg)
Calculated total radiation dose(uSv)	1.438	10.1	129.18
3.520		Average Accel Z(deg)	min gyroZ (deg)
Error	Total max and min for total flight	3.42	0
Gyro Z	Max GyroZ (deg)		
0.2	227.1	Stability ave for no gyro using our standardization	
uSv	min GyroZ (deg)	0.592765561	
0.7	0	Stability percantage +-60 degrees before stablization	
Pressure (Pa)	Max uSv (deg)	98	
100	4.62	Stability percantage error	
Humdity	Min uSv (deg)	20	
0.02	0	Stability percantage +-60 degrees before stablization	
Giger cpm		99.79	
0.8		Stability percantage error	
Accel Z (deg)		20	
0.04		Stability percantage +-60 degrees before stablization	
Temp(C)		#DIV/0!	
0.004		Stability percantage error	
		20	

[8.3.1]

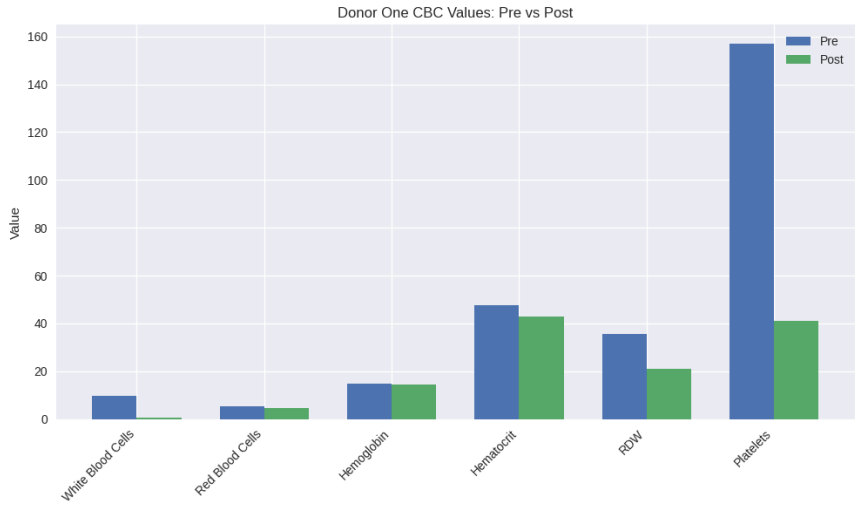

Donor ones (female) pre and post flight blood analysis

[8.3.1]

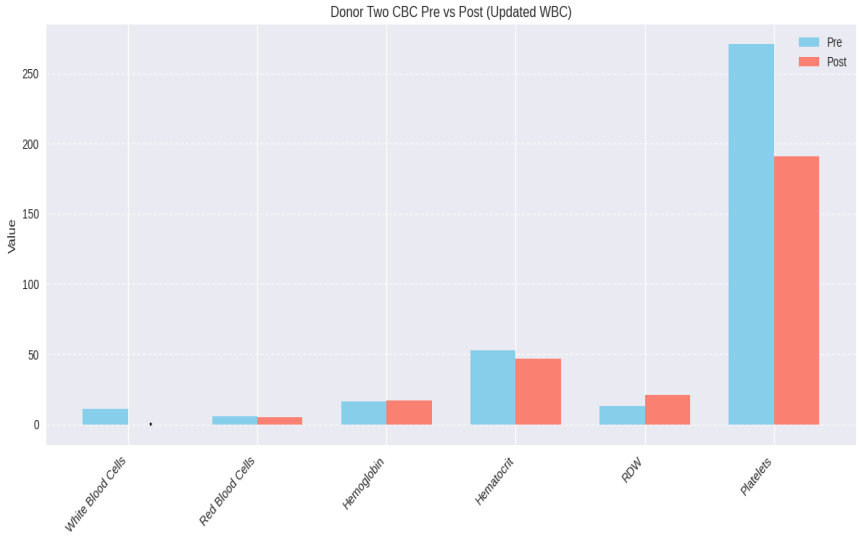

Donor twos (male) pre and post flight blood analysis

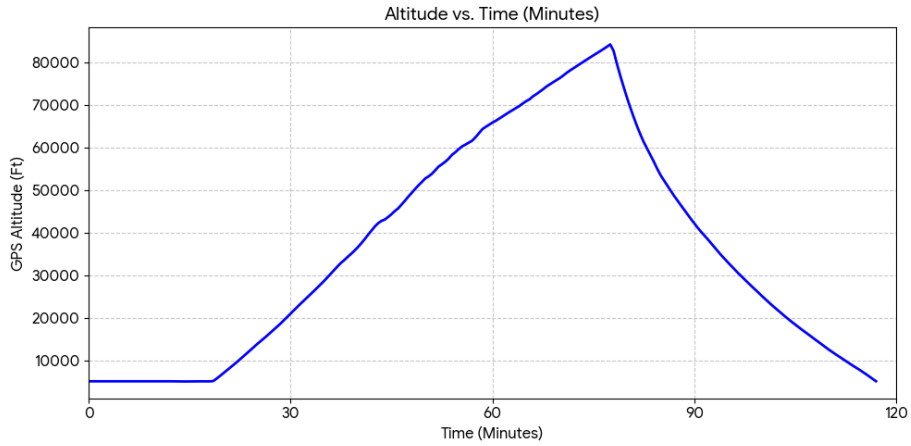

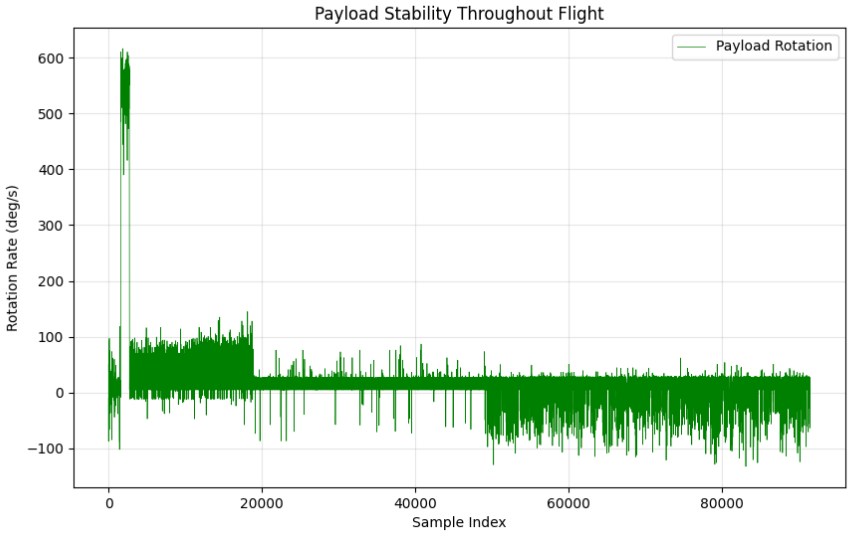
Payload Stability Throughout Flight
Payload Rotation
Rotation Rate (deg/s)
600
500
400
300
200
100
0
−100
0
20000
40000
60000
80000
Sample Index

[9.0] References

National Aeronautics and Space Administration. (2022, February 25). Scientists find increased red blood cell destruction during spaceflight. https://www.nasa.gov/mission_pages/station/research/news/find-increase-red-blood-cell-destruction

Federal Aviation Administration. (2023). Advisory Circular 450.31-1: Applying for FAA Determination on Policy or Payload Reviews. https://www.faa.gov/documentLibrary/media/Advisory_Circular/AC_450.31-1.pdf

Office of the Assistant Secretary for Preparedness and Response. Biosafety Level Requirements. https://aspr.hhs.gov/S3/Pages/Biosafety-Level-Requirements.aspx

Supawat, B., et al. (2022). Effects of low-dose radiation on human blood components after in vitro exposure to gamma radiation from ^{137}Cs radioactivity. Applied Radiation and Isotopes, 192, 110577. https://doi.org/10.1016/j.apradiso.2022.110577

Prades-Sagarra, E. (2024). Understanding the impact of radiation-induced lymphopenia: Preclinical and clinical research perspectives. Clinical and Translational Radiation Oncology, 49, 100852. https://doi.org/10.1016/j.ctro.2024.100852

Zare, A., & Mohammad Javad. (2020). The efficacy of periodic complete blood count tests in evaluation of the health status of radiation workers in Iran: A systematic review. Iranian Journal of Public Health, 49(4), 628. https://www.ncbi.nlm.nih.gov/pmc/articles/PMC7283191/

National Library of Medicine. (1999, September 1). Summary of health effects of ionizing radiation. Agency for Toxic Substances and Disease Registry (US). https://www.ncbi.nlm.nih.gov/books/NBK597567/

Kim, H., et al. (2016). Optimal radiation dose for patients with one to three lymph node positive breast cancer following breast-conserving surgery and anthracycline plus taxane-based chemotherapy: A retrospective multicenter analysis (KROG 1418). Oncotarget, 8(1), 1796–1804. https://doi.org/10.18632/oncotarget.12882

Trudel, G., Shahin, N., Ramsay, T., Laneuville, O. & Louati, H. (2022). Hemolysis contributes to anemia during long-duration space flight. Nature Medicine. https://www.nature.com/articles/s41591-021-01637-7?

National Weather Service. (n.d.). Weather balloon poster. https://www.weather.gov/media/key/KEY%20-%20Weather%20Balloon%20Poster.pdf

University of Colorado Boulder, Colorado Space Grant Consortium. (2025). Measuring Radiation with Respect to Altitude Using Kevlar Shielding, Non-Oxidizing Heating Agents for Stratospheric Operation of Thermal Sensitive Equipment, and Live Data Transmission. https://www.colorado.edu/center/spacegrant/media/1112

Agency for Toxic Substances and Disease Registry (US). (2019). Overview of basic radiation physics, chemistry, and biology (in Toxicological profile for thorium). National Library of Medicine Bookshelf. https://www.ncbi.nlm.nih.gov/books/NBK591329/

Occupational Safety and Health Administration. (n.d.). Introduction to ionizing radiation: Handout (Lecture outline). U.S. Department of Labor. https://www.osha.gov/ionizing-radiation/introduction/handout

University of Colorado Boulder, Colorado Space Grant Consortium. (2023). *2023 The Effect of Solar and Cosmic Radiation on Viscosity and pH of Pig Blood*. https://www.colorado.edu/center/spacegrant/media/458

University of Colorado Boulder, Colorado Space Grant Consortium. (2025). *Self-orienting payload for weather balloons*. https://www.colorado.edu/center/spacegrant/media/1117